JCTC Journal of Chemical Theory and Computation

ARTICLE

pubs.acs.org/JCTC

DFT and Ab Initio Study of Iron-Oxo Porphyrins: May They Have a Low-Lying Iron(V)-Oxo Electromer?

Mariusz Radoń,*[,†] Ewa Broclawik,[‡] and Kristine Pierloot[§]

[†]Faculty of Chemistry, Jagiellonian University, ul. Ingardena 3, 30-060 Kraków, Poland

[‡]Institute of Catalysis and Surface Chemistry, Polish Academy of Sciences, ul. Niezapominajek 8, 30-239 Kraków, Poland

[§]Department of Chemistry, University of Leuven, Celestijnenlaan 200F, B-3001 Heverlee-Leuven, Belgium

Supporting Information

ABSTRACT: The energetics of various electromeric states for two heme complexes with an iron-oxo (FeO^{3+}) group, $FeO(P)^{+}$ and FeO(P)Cl (P = porphin), have been investigated, employing DFT and correlated ab initio methods (CASPT2, RASPT2). Our interest focused in particular on tri- and pentaradicaloid iron(IV)-oxo porphyrin radical states as well as iron(V)-oxo states. Surprisingly, the iron(V)-oxo ground state is predicted for both models *in vacuo*. However, the presence of a polarizable medium, such as a solvent or a protein environment, favors the iron(IV)-oxo porphyrin radical cation, which is predicted to be the actual ground state of FeO(P)Cl under such conditions. Nonetheless, the iron(V)-oxo electromer is still expected to lie only a few kcal/mol above the ground state—a conclusion coming from both CASPT2 and RASPT2 calculations with a very large active space and further supported by a calibration with respect to coupled cluster CCSD(T) calculations for a simplified small model. The DFT results turn out to be strongly functional-dependent and thereby inconclusive. The widely used B3LYP functional—although correctly predicting the iron(IV)-oxo porphyrin radical ground state for FeO(P)Cl—seems to place the iron(V)-oxo states much too high in energy, as compared to the present CASPT2, RASPT2, and CCSD(T) results.

1. INTRODUCTION

High-valent iron-oxo porphyrins are strong and important oxidants, employed by nature in the cytochrome P450 catalytic cycle[1,2] and supposedly participating in the oxygen-transfer reactions catalyzed by iron porphyrins.[3] In both catalytic cycles, the active intermediate is normally assumed to be an iron(IV)-oxo porphyrin radical cation species, ($Fe^{IV}O$)($P^{\bullet+}$), also known as Compound I (Cpd I).[1] The high (+IV) oxidation state on Fe is stabilized by the coordination of strong electron donors: the porphyrinate and, particularly, the oxo ligand. In the presence of σ donors stronger than porphyrin (and more resistant to oxidation), such as tetradentate amido macrocycles, an even higher (+V) oxidation state of iron is stable in several known iron(V)-oxo complexes.[4,5] The possibility of iron(V)-oxo complexes with corroles and corrolazines (close analogues of porphyrins) was also reported.[6] All of these facts raise the important question of whether similar iron(V)-oxo species with a porphyrin ligand may also exist and be stable enough to be interesting for chemistry.[7,8] Due to the very electrophilic nature of the $Fe^{V}O$ group (d^3), the hypothetical iron(V)-oxo porphyrin species could be extremely strong oxidants, with possibly very interesting properties.

The hypothetical iron(V)-oxo porphyrin may be viewed as an electromer (electronic isomer) of the "standard" Cpd I—i.e., iron(IV)-oxo porphyrin radical—species, obtained by moving one electron from the iron to the porphyrin, as illustrated in Figure 1. Furthermore, as shown in this figure, in both the iron(IV) and iron(V) forms, two local spin states on iron should be considered. For the iron(IV)-oxo states, these two possibilities are usually referred to as *triradicaloid* (local triplet state on the Fe, denoted $^3Fe^{IV}$; three unpaired electrons in total) and *pentaradicaloid* (local quintet state on the Fe, denoted $^5Fe^{IV}$; five unpaired electrons in total). Similarly, for the iron(V)-oxo states, both the doublet and the quartet spin state are possible. The ligand radical in the triradicaloid and pentaradicaloid forms may be localized in either of the two highest-occupied π orbitals of the porphyrin ($P\pi$): a_{2u} or a_{1u} (the scheme in Figure 1 shows the first possibility).[9] For each type of ligand radical, the coupling between the local spin on iron (triplet or quintet) and the local spin on the ligand (doublet) may be either ferro- or antiferrmagnetic, thus producing a pair of close-lying electronic states: quartet and doublet (for the triradicaloid form) or sextet and quartet (for the pentaradicaloid form). Therefore, there are plenty of possible iron(IV) and iron(V) electronic states to be considered. Each of these states will be labeled by specifying the oxidation state and the local spin on the iron (e.g., $^3Fe^{IV}$, $^4Fe^{V}$) as well as the radical character and the local spin on the porphyrin: either closed-shell ^1P or the radical cation $^2P^{\bullet+}$ of two types (a_{2u} or a_{1u}); this notation is used in Figure 1.[10]

Various spectroscopic techniques have clearly identified the triradicaloid iron(IV)-oxo ground state for Cpd I species of enzymes and their synthetic analogues.[11−16] A consensus has been reached between experiment and theory about this description.[1] Nonetheless, there have also been remarkable arguments in favor of iron(V)-oxo porphyrin species: from an early (and maybe naive) notion in the 1990s[17,18] until the dissemination of recent spectroscopic data from laser flash photolysis (LFP)

Received: October 28, 2010
Published: March 23, 2011

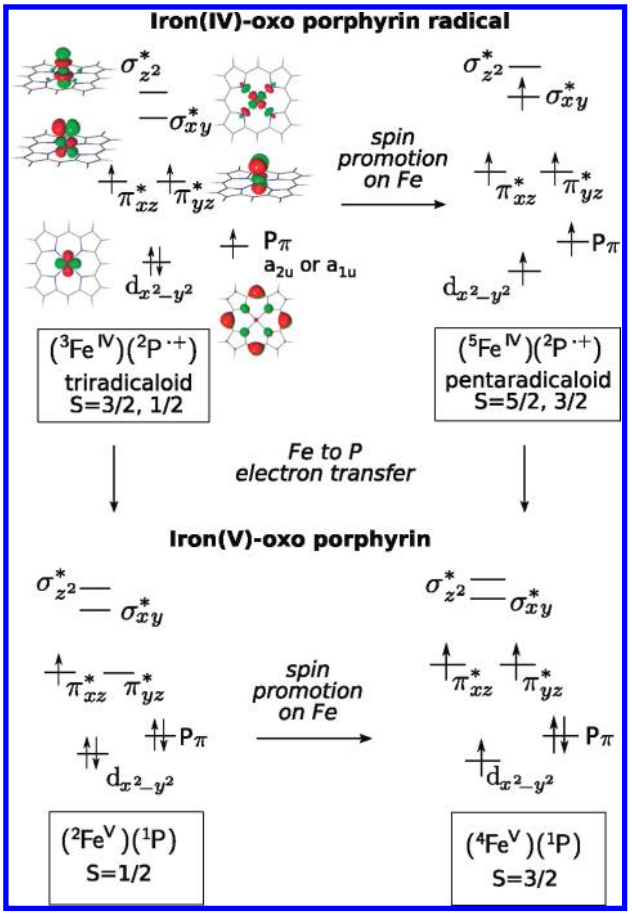

Figure 1. Electronic structure of an iron-oxo porphyrin compound in its various possible electromeric states.

experiments.[19−21] The LFP experiments seem to suggest that the iron(V)-oxo electromer could be stable enough to be "seen" in UV/vis spectroscopy and kinetic experiments, and it was even speculated that the iron(V)-oxo species may play some role in oxo-transfer reactions catalyzed by iron porphyrins and enzymes.[21] Yet, theory was rather sceptical of this concept. The iron(V)-oxo electromer of the P450 Cpd I model was indeed captured in some of the DFT studies, but at such a high energy (16−24 kcal/mol) above the iron(IV)-oxo triradicaloid ground state that it was judged as not likely to play any role in the catalytic oxidation pathways.[22,23] Only very recently, Chen et al.[24] showed that with multireference ab initio methods (CASPT2) the iron(V)-oxo states appear at lower energies, suggesting that they might be readily accessible at ambient temperatures. Moreover, on the basis of recent theoretical studies, the iron(IV)-oxo pentaradicaloids were also proposed as alternative active species in the catalytic cycle.[23,24] Despite notable progress, little is still known about the stabilities of various electromeric states in high-valent iron-oxo porphyrins (also in general, not necessarily restricted to models of P450 Cpd I). In our opinion, some aspects of the computational methodology also have to be further clarified, such as the performance of DFT and the adequacy of the active spaces used in the multireference calculations reported so far[24−27] (in particular, the π system of porphyrin) in providing a realistic description of the various electromeric states. We note that a reliable theoretical description of Cpd I and related iron-oxo species really is a challenging task for all computational methods, having to

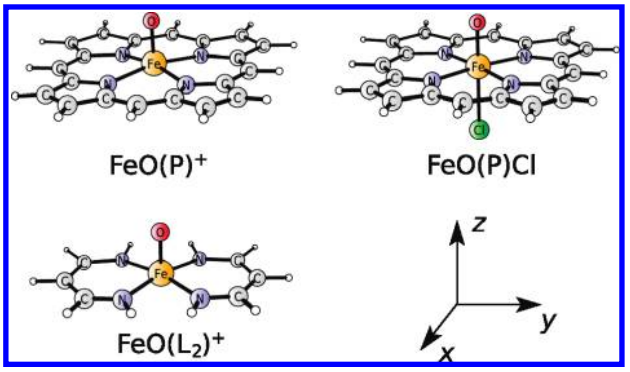

Figure 2. Structures of the studied heme complexes $(FeO(P)^+$, FeO(P)Cl) and of the small model $(FeO(L_2)^+)$, and their orientation in the coordinate system.

deal with at least two tricky issues: the problem of noninnocent ligands on the one hand and the description of spin state energetics in transition metal complexes on the other hand.[8]

In this paper, we study the relative energies of various electromeric states in two model iron-oxo porphyrin complexes: $FeO(P)^+$ and FeO(P)Cl (P = porphin), shown in Figure 2. The complexes are studied using quantum-chemical calculations *in vacuo*, but the effects of a polarizable environment are also investigated. In addition to (now standard) DFT methods, we apply a multireference ab initio formalism: both the Complete Active Space (CASSCF/CASPT2) method[28] and its generalization—the Restricted Active Space (RASSCF/RASPT2) methods.[29] The RASPT2 method permits us to include more active orbitals in the active space than is possible in CASPT2, in particular, to extend the active space with a number of porphyrin π orbitals. On the basis of our previous experience with copper corroles[30] (also dealing with the question of metal versus ligand-based oxidation), the latter orbitals are expected to significantly influence the splitting between the iron(V)-oxo and iron(IV)-oxo porphyrin radical electromers. While considering various computational approaches for the present problem, we also thought about the coupled cluster CCSD(T) method. However, as the presently studied heme complexes are too large for this method, we applied CCSD(T) to a smaller model complex, $FeO(L_2)^+$ (where L = η^2-$N_2C_3H_5^-$ is the vinylogous amidine ligand), designed to mimic the essential structural and electronic features of the heme complexes, as shown in Figure 2. The idea of such a small model was inspired by similar "calibration" studies by Harvey et al. on ferrous and ferric heme systems.[31,32] As we shall see, cross-checking of DFT, RASPT2, and CCSD(T) for the small model gives extra knowledge about the performance of these methods for the present task.

2. COMPUTATIONAL DETAILS

2.1. DFT Calculations. Spin-unrestricted DFT calculations were carried out with the Turbomole 5.9[33] and Gaussian 2009[34] packages, employing the def2-TZVP basis sets.[35] To cover a broad spectrum of various exchange-correlation functionals, we used both popular hybrid (B3LYP,[36] PBE0,[37] B3LYP*[38]) and nonhybrid functionals (BP86,[39,40] PBE,[41] OLYP[42]). We also tried the recently developed long-range corrected hybrid functional (LC-ωPBE[43−46]), hoping that it might improve the description of electron transfer between the iron and porphyrin fragments. The structures were optimized at the BP86 level for

each of the considered electronic states (adiabatic calculations). DFT:BP86 structures were used in single point calculations with all other functionals (since initial tests showed that the relative energies are changing by just a fraction of a kcal/mol as compared to the energies obtained from full structure optimizations with each functional). The optimizations performed for the heme complexes exploited their C_{4v} symmetry, except for the degenerate $^2Fe^V$ doublet, which has an unequal occupation of the FeO $\pi^*_{xz,yz}$ orbitals and thus undergoes a significant Jahn−Teller distortion to C_{2v}. The distortion is more pronounced for FeO(P)$^+$ than for FeO(P)Cl. In order to preserve the similarity with the heme complexes, the small model was optimized with its four nitrogens constrained to lie in a single plane. The optimized Cartesian coordinates may be found in the Supporting Information. A number of DFT calculations including implicit solvation were also performed, making use of the standard COSMO model[47] as implemented in Turbomole. These calculations were performed for two values of the dielectric constant (ε = 5.7 and 79), using the (unoptimized) bond radii multiplied by 1.17, and all other settings set as the defaults in Turbomole 5.9. Selected test calculations were also repeated with the PCM model[48] as implemented in Gaussian 2009. Very similar effects of solvation were obtained with both solvation models.

2.2. CASSCF/CASPT2 and RASSCF/RASPT2 Calculations. CASSCF/CASPT2[28] and RASSCF/RASPT2[29] calculations were performed with Molcas 7.4,[49] using a scalar-relativistic second-order Douglas−Kroll Hamiltonian,[50] the standard IPEA-shifted zero order Hamiltonian for second order perturbation theory,[51] and Cholesky decomposition of two-electron repulsion integrals[52]—all of these features as implemented in Molcas 7.4. Single-point calculations were performed on top of the DFT:BP86 structures obtained for each electronic state. The calculations for the heme complexes employed two types of Atomic Natural Orbitals (ANO) basis sets (basis I and II). The smaller one (basis I) was composed of ANO-RCC[53] on iron (contracted to [7s6p5d2f1g]) and ANO-S[54] on the ligands (contracted to [4s3p1d] on C, N, and O, to [5s4p2d] on Cl, and to [2s] on H). The larger one (basis II) was composed of ANO-RCC on all atoms, contracted to [7s6p5d3f2g1h] on Fe; to [4s3p2d1f] on C, N, and O; to [5s4p3d2f] on Cl; and to [3s1p] on H. The results reported in section 3 were obtained with basis II, while basis I was used mostly for testing purposes (see the Supporting Information). The calculations for the small model FeO(L$_2$)$^+$ additionally employed three types of correlation consistent basis sets, the same as used in the CCSD(T) calculations and denoted as T/D, T/T, and Q/T (*vide infra*). In all CASPT2 and RASPT2 calculations, the core electrons were kept frozen. However, for bases I and II, the semicore Fe (3s, 3p) electrons were correlated, in contrast to the correlation consistent basis sets (T/D, T/T, Q/T), which are not designed for correlating these electrons. It was tested (with basis I) that excluding the Fe (3s, 3p) electrons from the correlation treatment only gives a secondary difference in the relative energies (affecting mostly the energy difference between the pentaradicaloid and triradicaloid Fe^{IV} states, while leaving the separation between the Fe^V and Fe^{IV} states virtually unaffected).

All of the CASSCF/CASPT2 and RASSCF/RASPT2 calculations were performed state specifically for each of the considered electronic states. The high symmetry of the present models (C_{4v} for the heme models, C_{2v} for the small model) is beneficial for locating the interesting states as the lowest CI roots corresponding to a given spin and spatial symmetry. Actually, due to technical limitations (Molcas supports Abelian groups only), all of the calculations were performed in C_{2v} formal symmetry. Most of the considered electronic states were still located as the lowest roots in different irreps of C_{2v}. This is not the case with the $^4A_2$ and $^4B_2$ states, both belonging to the same irrep (A_2) in C_{2v}. However, as they are still orthogonal, the $^4A_2$ and $^4B_2$ states were easily distinugished from each other in state-specific calculations (with help of the CISELECT facility of the RASSCF module in Molcas). Obviously, it would be more difficult to apply the same state-specific procedure to less symmetric systems (not covered in this study), like for instance P450 Cpd I. In general, symmetry lowering may cause mixing between the Fe^{IV} and the Fe^V states, analogous that found here for the $^2B_1$ state of the small model (*vide infra*).

The choice of the active orbitals for the CASSCF calculations was made according to the standard rules for transition metal compounds.[55−57] Nondynamical correlation effects involving the Fe 3d electrons, the Fe−O bond, and the Fe−P σ bond are described by making active four pairs of bonding−antibonding orbitals ($Fe3d_{xz}-O2p_x \rightarrow (\pi_{xz},\pi^*_{xz})$; $Fe3d_{yz}-O2p_y \rightarrow (\pi_{yz},\pi^*_{yz})$; $Fe3d_{z^2}-O2p_z \rightarrow (\sigma_{z^2},\sigma_{z^2}{}^*)$; $Fe3d_{xy}-P\sigma_{xy} \rightarrow (\sigma_{xy},\sigma^*_{xy})$), the remaining nonbonding Fe $3d_{x^2-y^2}$ orbital, and three double-shell orbitals ($3d'_{xz}$, $3d'_{yz}$, $3d'_{x^2-y^2}$). In order to allow electron transitions between the Fe and P fragments, the two highest-occupied π orbitals of the porphyrin, $a_{2u}(a_1)$ and $a_{1u}(a_2)$, as well as their correlating π^* orbitals $e_g(b_1,b_2)$ were made active. These four frontier π orbitals of the porphyrin are known in the literature as the *Gouterman set*. This choice leads to an active space of 15 electrons distributed in 16 active orbitals (15in16). Although this is already a fairly large active space, previous experience[58] tells us that many more (preferably all) π, π^* orbitals on porphyrin should be made active in order to provide a correct description of the relative energies of various electromeric states (in particular, the Fe^V and Fe^{IV} states). Obviously, this is computationally not feasible within CASSCF. Therefore, RASSCF calculations were performed instead. Here, the active space is further subdivided into three subspaces, RAS1, RAS2, and RAS3.[29] The RAS2 subspace (where, as in CASSCF, all possible excitations are allowed) was kept limited to the singly occupied orbitals plus those pairs of orbitals describing the most important nondynamical correlation effects. In contrast, the doubly occupied π orbitals of the porphyrin and their correlating π^* orbitals, as well as other less important active orbitals (among which the three 3d′ orbitals), were kept in RAS1 (if nearly doubly occupied) or in RAS3 (if nearly empty). Up to double excitations were then allowed out of RAS1 and into RAS3. Similar calculations have already been performed recently, both for organic molecules (such as free base porphin) and transition metal systems (such as copper corrole).[29,30,58] However, for the present case, it turned out to be particularly difficult to find a combination of a global active space with an RAS2 subspace that is both reliable and still computationally feasible. A number of test calculations have been carried out for this purpose: selected results are given in the Supporting Information, and the most important conclusions obtained from these preliminary studies are summarized below.

First, extending the 15in16 active space with all remaining π and π^* orbitals of the porphyrin leads to a very large active space of 37 electrons in 36 orbitals (37in36). This active space is computationally feasible only if combined with a very small RAS2 subspace, containing only the singly occupied (SO) orbitals. Therefore, 37in36 was reduced by removing four occupied π orbitals of the porphyrin and their four correlating π^* orbitals

(eight orbitals in total). The orbitals removed correspond to combinations of C2p$_z$ of the β carbons of the pyrrole rings. The resulting active space of 29 electrons in 28 orbitals (29in28) still contains 16 (π,π^*) orbitals on the porphyrin and may be viewed as an active space correlating 18 "aromatic electrons" of the porphyrin ring (Hückel formula: $4n + 2 = 18$ for $n = 4$, corresponding to the shortest cyclic path through the porphyrin ring). A comparison of the results obtained with the 37in36 and 29in28 active spaces, combined with a RAS2 subspace containing only the singly occupied orbitals, has shown that both active spaces point to a similar (up to ±3 kcal/mol) set of relative energies (see the Supporting Information).

The second step was to find a reasonable RAS2 subspace to be combined with the 29in28 global active space. To this end, various choices of RAS2 were compared within the smaller 15in16 global active space (see the Supporting Information). First, it turns out that a RASPT2(15in16) treatment based on a RAS2(15in11) subspace (i.e., with the Fe 3d′ and the correlating π^* (e_g) orbitals on the porphyrin moved to RAS3 as compared to CAS) produces nearly the same relative energies as the full CASPT2(15in16) treatment. This brings a promising suggestion that both the 3d double-shell effect on iron and the porphyrin $\pi-\pi^*$ correlation may be well described by up to double excitations. Next, RASPT2(15in16) calculations were tested in combination with two smaller subspaces, denoted as RAS2(6+SO) and RAS2(8+SO). RAS2(6+SO) contains three couples of bonding−antibonding Fe3d−O2p orbitals and all (remaining) singly occupied orbitals (i.e., 7in6 for ^{2}E, 9in7 for ^{4}A$_{1,2}$, 11in9 for ^{6}A$_{1,2}$). With this RAS2 space, an optimal description of the nondynamical correlation effects connected to the (very covalent) Fe−O bond is provided. RAS2(8+SO) additionally contains the σ_{xy},σ^*_{xy} pair, thus improving the description of nondynamical correlation related to σ donation from P to Fe. Obviously, the RASPT2 results obtained with RAS2(6+SO) and RAS2(8+SO) differ somewhat from each other and from those obtained with RAS2(15in11), as well as from the full CASPT2 results. However, the differences are rather small (a few kcal/mol), indicating that even the least extensive subspace RAS2(6+SO) is a reasonable choice. The results reported below refer to the 29in28 global active space combined with the RAS2(6+SO) subspace. The choice of RAS2(8+SO) would perhaps give slightly better results. However, this subspace is too large to be combined with the 29in28 global space at a reasonable computational cost. The small variation of the relative energies caused by excluding the σ_{xy},σ^*_{xy} pair from RAS2 in RAS2(6+SO) is not expected to change any of our important conclusions below.

The active space for the small model was constructed analogously. Since we have not found any natural analogue of the Goutermann π set for the small model, the 15in16 active space was not considered, and hence no CASSCF/CASPT2 calculations were performed for the small model. Including all ligand π and π^* orbitals gives an active space of 23 electrons in 22 orbitals (23in22) for RASSCF/RASPT2 calculations. This active space is still small enough to be combined with various choices of RAS2 (defined analogously as for the heme models): RAS2(6+SO), RAS2(8+SO), and RAS2(15in11). (The last subspace contains the highest occupied π orbitals of a$_1$ and b$_2$ symmetries instead of a$_{2u}$ and a$_{1u}$ for porphyrin.) The orbital carrying the free radical in the Fe^{IV} states considered for the small model, HOMO(b$_2$), was treated as singly occupied not only for the ^{4}B$_1$ and ^{6}B$_2$ states but also for ^{2}B$_1$, where it is partially occupied due to the mixed Fe^V−Fe^{IV} character of this state (*vide infra*). In contrast, this orbital was treated as doubly occupied for the ^{2}B$_2$ state. Our main conclusions drawn from these test calculations essentially confirm the picture obtained for the heme complexes. Thus, the 23in22 results obtained with RAS2(15in11) and RAS2(8+SO) are nearly identical and also similar to those obtained with the RAS2(6+SO) subspace. The largest discrepancies between the RAS2(6+SO) and RAS2(8+SO) subspaces are observed for the tri- to pentaradicaloid excitation energy. However, we shall see that the CASPT2/RASPT2 description of this excitation is almost certainly biased in favor of the high-spin state anyway. In contrast, the difference between the predicted Fe^V−Fe^{IV} gaps with both RAS2 spaces is much less pronounced. The results reported for the small model in section 3 refer to the 29in28 global active space with a RAS2(8+SO) subspace. More technical details of CASSCF/CASPT2 and RASSCF/CASPT2 calculations may be found in the Supporting Information.

2.3. CCSD(T) Calculations for the Small Model. Restricted open-shell CCSD(T) calculations were performed for DFT: BP86 structures with Molpro 2009[59] using the Douglas−Kroll (DK) scalar relativistic Hamiltonian and three DK recontractions[60] of the Dunning correlation consistent (cc) basis sets.[61] The smallest one, denoted T/D, was composed of cc-pVTZ-DK on Fe and cc-pVDZ-DK on the ligands. The middle one, T/T, was simply cc-pVTZ-DK on all atoms. The most extensive one, Q/T, was composed of cc-pVQZ-DK on Fe and cc-pVTZ-DK on the ligands. The correlation energy extrapolated to the complete basis set on Fe (while keeping cc-pVTZ-DK on the ligands) was also calculated from the Q/T and T/T results assuming the "1/X^3" dependence of the residual correlation energy due to Helgaker et al.[62]—yielding the results reported below as ∞/T. The restricted open-shell Kohn−Sham orbitals obtained from the B3LYP functional were used in the CCSD(T) calculations in order to speed up the coupled cluster convergence and to reduce the orbital bias caused by electron correlation (for the use of Kohn−Sham orbitals in coupled cluster calculations, we refer to the literature[32,63−65]). The impact of multireference effects on the coupled cluster calculations was estimated by means of various diagnostics computed for the CCSD wave function: $\mathscr{T}_1$,[66] $\mathscr{D}_1$,[67] and the maximum absolute value found for the amplitudes of double-excitations ($\max_{ij,ab}|t_{ij}^{ab}|$).

3. RESULTS AND DISCUSSION

3.1. Electromeric States of FeO(P)$^+$ and FeO(P)Cl. Before discussing the stability of various electromeric forms for the heme models, FeO(P)$^+$ and FeO(P)Cl, let us first describe which of their electronic states are included in this study. The various electromeric forms (cf Figure 1) give rise to the following electronic states (all labeled under C_{4v} symmetry):

$$(^3\mathrm{Fe^{IV}O})(^2\mathrm{P^{\bullet+}}a_{2u}) \rightarrow {}^2\mathrm{A}_2 + {}^4\mathrm{A}_2$$

$$(^3\mathrm{Fe^{IV}O})(^2\mathrm{P^{\bullet+}}a_{1u}) \rightarrow {}^2\mathrm{A}_1 + {}^4\mathrm{A}_1$$

$$(^5\mathrm{Fe^{IV}O})(^2\mathrm{P^{\bullet+}}a_{2u}) \rightarrow {}^4\mathrm{A}_1 + {}^6\mathrm{A}_1$$

$$(^5\mathrm{Fe^{IV}O})(^2\mathrm{P^{\bullet+}}a_{1u}) \rightarrow {}^4\mathrm{A}_2 + {}^6\mathrm{A}_2$$

$$(^2\mathrm{Fe^{V}O})(^1\mathrm{P}) \rightarrow {}^2\mathrm{E}$$

$$(^4\mathrm{Fe^{V}O})(^1\mathrm{P}) \rightarrow {}^4\mathrm{B}_2$$

Table 1. Relative Energies (kcal/mol) of the Low Lying Electronic States of $FeO(P)^{+}$[a]

		B3LYP	B3LYP*	OLYP	BP86	CASPT2[b]	RASPT2[c]
$(^3Fe^{IV}O)(^2P^{\bullet+}a_{2u})$	$^4A_2$	0	0	0	0	0	0
	$^2A_2$	0.4	0.4	0.4	0.4	−0.6	0.4
$(^3Fe^{IV}O)(^2P^{\bullet+}a_{1u})$	$^4A_1$	−3.3	−2.8	−1.2	−1.5	6.4	−0.7
	$^2A_1$	−3.4	−2.9	−1.1	−1.3	5.6	−0.6
$(^5Fe^{IV}O)(^2P^{\bullet+}a_{2u})$	$^6A_1$	8.9	12.4	9.7	19.1	3.9	0.1
$(^5Fe^{IV}O)(^2P^{\bullet+}a_{1u})$	$^6A_2$	5.7	9.9	9.1	18.3	11.2	−0.8
$(^2Fe^{V}O)(^1P)$	^2E	12.7	9.2	0.5	−2.4	−3.4	−6.5
$(^4Fe^{V}O)(^1P)$	$^4B_2$	12.8	11.3	3.4	5.7	−1.6	−3.5

[a] CASPT2 and RASPT2 energies obtained with basis II, DFT energies with def2-TZVP (see section 2). [b] Based on the 15in16 active space, including only the four π (Gouterman) orbitals on the porphyrin. [c] Based on the 29in28 active space, including 16 π orbitals on the porphyrin, with RAS2(6+SO).

Table 2. Relative Energies (kcal/mol) of the Low Lying Electronic States of FeO(P)(Cl)[a]

		B3LYP	B3LYP*	OLYP	BP86	CASPT2[b]	RASPT2[c]
$(^3Fe^{IV}O)(^2P^{\bullet+}a_{2u})$	$^4A_2$	0	0	0	0	0	0
	$^2A_2$	0.1	0.1	0.1	0.1	−1.4	0.0
$(^3Fe^{IV}O)(^2P^{\bullet+}a_{1u})$	$^4A_1$	6.3	6.8	8.0	8.1	16.5	9.1
	$^2A_1$	5.8	6.4	7.8	7.9	15.5	9.0
$(^5Fe^{IV}O)(^2P^{\bullet+}a_{2u})$	$^6A_1$	9.7	12.9	10.1	19.1	3.2	−1.5
$(^5Fe^{IV}O)(^2P^{\bullet+}a_{1u})$	$^6A_2$	17.1	20.7	18.7	27.8	21.1	9.6
$(^2Fe^{V}O)(^1P)$	^2E	12.4	13.3	2.9	1.0	1.6	−1.7
$(^4Fe^{V}O)(^1P)$	$^4B_2$	13.1	11.5	3.5	5.9	3.1	2.8

[a] CASPT2 and RASPT2 energies obtained with basis II, DFT energies wih def2-TZVP (see section 2). [b] Based on the 15in16 active space, including only the four π (Gouterman) orbitals on the porphyrin. [c] Based on the 29in28 active space, including 16 π orbitals on the porphyrin, with RAS2(6+SO).

Due to the high symmetry of the heme complexes, mixing between most of the listed electronic states is symmetry-forbidden. Exceptions are the quartets of $A_{1,2}$ symmetry, each emerging both from the triradicaloid and the pentaradicaloid form. However, because of the different local spin on the iron for both forms, virtually no mixing is observed in this case. We further note that for the pentaradicaloid form $(^5Fe^{IV})(^2P^{\bullet+})$, only the sextet states will be reported below (the corresponding quartet states are expected to have very similar energies[24]).

Tables 1 and 2 contain the relative (adiabatic) energies obtained for the considered states of the studied heme complexes, $FeO(P)^{+}$ and FeO(P)Cl; in all cases, the energies are given with respect to $^4A_2$ (i.e., the triradicaloid with a_{2u} hole).

Let us first focus on the iron(IV)-oxo triradicaloid states. As might be expected, the doublet and the quartet states of each triradicaloid (a_{2u}- or a_{1u}-type) are close in energy—a situation which is also known well for the models of P450 Cpd I.[1,68] Looking at the relative energies of the states with either a_{2u} or a_{1u} orbitals singly occupied (i.e., considering the $^4A_2-{}^4A_1$ or $^2A_2-{}^2A_1$ gap), one may easily notice that the different DFT methods predict rather similar relative energies, which are also close to the RASPT2 results. In contrast, the CASPT2 calculations significantly overstabilize the a_{2u}-type radicals. This is obviously caused by the limitations of the 15in16 active space underlying the CASPT2 calculations; this active space includes only four frontier π orbitals on the porphyrin (the Gouterman set). The deficiency is clearly removed in the RASPT2 calculations based on the larger 29in28 active space, containing now as many as 16 π orbitals on the porphyrin. We further notice that the a_{1u}-type radicals ($^{2,4}A_1$) are more stable than the a_{2u}-type radicals ($^{2,4}A_2$) for $FeO(P)^{+}$ (except for the deficient CASPT2 calculations), whereas in FeO(P)Cl, this ordering is reversed. It was noted just above that within the same configuration (either a_{1u} or a_{2u} radical), a very small quartet−doublet energy separation is found at all computational levels. This is easily understandable, as both states differ only by weak magnetic coupling between two spatially separated spins: on the FeO group and on the porphyrin. However, from the results in Tables 1 and 2, it is clear that also for this property CASPT2 gives results that are deviating both from the DFT and the RASPT2 results, by overestimating the absolute value of the magnetic coupling and often giving it a wrong sign (i.e., predicting antiferromagnetic instead of ferromagnetic coupling). Again, these deviating results should be brought back to the limitations of the 15in16 active space used in CASPT2. Using a larger active space, the RASPT2 calculations clearly provide results for the $^2A_2-{}^4A_2$ and $^2A_1-{}^4A_1$ gaps that are superior to those of CASPT2.

Let us now focus on the energy difference between the pentaradicaloid $(^5Fe^{IV})(^2P^{\bullet+})$ and the corresponding triradicaloid $(^3Fe^{IV})(^2P^{\bullet+})$ states. As was already mentioned (and is shown in Figure 1), the transition from the tri- to pentaradicaloid state *de facto* comes down to a spin promotion from the intermediate-spin (triplet) to the high-spin (quintet) local spin state of Fe^{IV}. Due to the local character of this excitation, about the same energy difference is obtained for the a_{2u}-type radicals (i.e., $^6A_1-{}^4A_2$ gap) as for the a_{1u}-type radicals (i.e., $^6A_2-{}^4A_1$ gap). It is known from previous studies on transition metal complexes[8,69−71] that spin state energetics are very sensitive to the applied DFT method. This is also the case here, the hybrid functionals predicting a much lower relative energy of the sextet (spin-promoted) state than the nonhybrid functionals. The discrepancies are substantial, for instance BP86 predicts the $^6A_1$ state at ∼19 kcal/mol above the $^4A_2$ state, while B3LYP gives only ∼9−10 kcal/mol. Considering the spin promotion energy, the OLYP (nonhybrid) functional performs closer to the hybrid than to other nonhybrid functionals, such as BP86 or PBE (the latter results are given in the Supporting Information). We next observe that the CASPT2 and RASPT2 calculations clearly favor the high-spin states, predicting even smaller promotion energies than those from the hybrid functionals. A similar result was also obtained by Chen et al. in their CASPT2/MM study of P450 Cpd I.[24] However, recent studies on a number of iron(II) complexes in N_4 and N_2O_2 architectures[72−74] have indicated that CASPT2 has a tendency to overstabilize the high spin (quintet) state in these systems with at least a few kcal/mol. All problematic cases involve an electron excitation from the nonbonding iron 3d orbital to the antibonding iron−ligand combination, $d_{x^2-y^2} \rightarrow \sigma^*_{xy}$. The same type of electron excitation is also involved here. We therefore suspect that the present CASPT2 results may be biased toward the pentaradicaloid states by a few kcal/mol, a problem that is clearly not solved by going to RASPT2. Further confirmation of this observation will be provided by comparing RASPT2 with CCSD(T) benchmark calculations for the small model (*vide infra*).

Perhaps the most exciting property of the studied complexes is the relative stability of the iron(V)-oxo and the iron(IV)-oxo

porphyrin radical electromers. As observed previously for the spin promotion energy, here also the DFT results turn out to be substantially functional-dependent. The hybrid functionals, like B3LYP, B3LYP*, and PBE0 (the latter results are given in the Supporting Information), strongly favor the iron(IV)-oxo triradicaloid states ($^{2,4}A_1$ or $^{2,4}A_2$) and predict a very high energy for the iron(V)-oxo states (^2E, $^4B_2$). In contrast, the nonhybrid functionals, like BP86, OLYP, and PBE, place both types of states within a few kcal/mol margin. Actually, BP86 and PBE predict the ^2E state as the ground state in $FeO(P)^+$ and as nearly degenerate with the (triradicaloid) ground state in FeO(P)Cl. Reducing the amount of HF exchange from 20 to 15% in the B3LYP* functional does bring the predictions of this functional somewhat closer to the nonhybrid functionals than is the case for B3LYP (although not always—see the ^2E state in FeO(P)Cl), but still the discrepancy is huge. We also applied the more recent, range-separated hybrid functional LC-ωPBE, hoping that it might improve the description of electron transfer between the iron and the porphyrin.[44] However, for the presently studied systems, this functional performs very similarly to the traditional hybrid functionals (the results may be found in the Supporting Information). In sum, we have found that the hybrid and nonhybrid functionals point to two completely different pictures, with differences in relative energies sometimes much larger than 10 kcal/mol. Which of these two pictures is then closer to reality?

The multireference RASPT2(29in28) and CASPT2(15in16) calculations rather unambiguously place the iron(V)-oxo states at low energy. This is qualitatively similar to the predictions from the nonhybrid functionals. Such a low energy for the iron(V)-oxo electromer may seem rather surprising. In fact, after performing the CASPT2(15in16) calculations, we initially suspected that the iron(V)-oxo states might be overstabilized by this method, given the limitations of the 15in16 active space. This was our primary motivation to introduce the extended 29in28 active space, by including more π,π^* orbitals on the porphyrin, and thereby improving the description of the electron transfer from the iron to the macrocycle. To our surprise, this enlargement of the active space turned out to stabilize the iron(V)-oxo states even more! In fact, the RASPT2 calculations predict an iron(V)-oxo ground state (^2E) for both complexes. This is the situation predicted for isolated molecules *in vacuo*; as will be shown below, the presence of solvent or another polarizable medium is important for the relative energetics and may even change the ground state. We note that in a recent CASPT2/MM study by Chen et al.,[24] the iron(V)-oxo electromer was also found at low energy for Cpd I of cytochrome P450. The authors of the cited paper used an active space analogous to our 15in16 space, though even slightly smaller on the porphyrin. We expect that extension of their active space (i.e., providing a more balanced description of charge transfer between the porphyrin and the FeO group) would even further stabilize the iron(V)-oxo electromer of Cpd I.

In previous DFT studies, the iron(V)-oxo states of P450 Cpd I were reported as electronically unstable in the presence of a polarizable continuum or of point charges (i.e., the SCF procedure under such conditions converging to the "usual" triradicaloid state).[2,22,23] Here, we estimated the effect of polarization on the relative energetics of various electromers by means of the standard COSMO model.[47] The calculations with a dielectric continuum obviously cannot provide a quantitative description of the $FeO(P)^+$ and FeO(P)Cl species in solution—their only purpose is to provide a qualitative estimation of (nonspecific) environmental effects in order to distinguish the situation *in vacuo* from the situation in solution or in a protein. The calculations employed two values for the dielectric constant: $\varepsilon = 5.7$ (corresponding to a weakly polar solvent such as chlorobenzene and often used for modeling the weakly polar interior of proteins) and $\varepsilon = 79$ (corresponding to a polar solvent—water) and were performed at the DFT level with two functionals: B3LYP and BP86. The estimated effects of the polarizable continuum on the relative energetics are given in Tables 3 and 4. The numbers provided in these tables are the differences in relative energy, with respect to the $^4A_2$ state, between the COSMO and the vacuum calculations.

Table 3. Effect of the Polarizable Continuum (COSMO) on the Relative Energetics in $FeO(P)^+$ (kcal/mol)

		$\varepsilon = 5.7$		$\varepsilon = 78$	
		B3LYP	BP86	B3LYP	BP86
$(^3Fe^{IV}O)(^2P^{\bullet+}a_{2u})$	$^4A_2$	0	0	0	0
$(^3Fe^{IV}O)(^2P^{\bullet+}a_{1u})$	$^4A_1$	0.0	0.2	0.0	0.2
$(^5Fe^{IV}O)(^2P^{\bullet+}a_{2u})$	$^6A_1$	0.6	0.4	0.8	0.6
$(^5Fe^{IV}O)(^2P^{\bullet+}a_{1u})$	$^6A_2$	0.2	0.3	0.2	0.3
$(^2Fe^{V}O)(^1P)$	^2E	2.7	2.3	3.7	3.2
$(^4Fe^{V}O)(^1P)$	$^2B_2$	1.5	1.5	2.2	2.1

Table 4. Effect of the Polarizable Continuum (COSMO) on the Relative Energetics in FeO(P)Cl (kcal/mol)

		$\varepsilon = 5.7$		$\varepsilon = 78$	
		B3LYP	BP86	B3LYP	BP86
$(^3Fe^{IV}O)(^2P^{\bullet+}a_{2u})$	$^4A_2$	0	0	0	0
$(^3Fe^{IV}O)(^2P^{\bullet+}a_{1u})$	$^4A_1$	−1.7	−1.9	−2.2	−2.5
$(^5Fe^{IV}O)(^2P^{\bullet+}a_{2u})$	$^6A_1$	1.1	0.9	1.6	1.3
$(^5Fe^{IV}O)(^2P^{\bullet+}a_{1u})$	$^6A_2$	0.0	−0.4	0.1	−0.3
$(^2Fe^{V}O)(^1P)$	^2E	5.7	5.6	7.9	7.9
$(^4Fe^{V}O)(^1P)$	$^2B_2$	4.4	3.4	6.2	4.9

First, it can be seen that both functionals—even though predicting very different relative energetics (cf. Tables 1 and 2)—now point to quite similar "solvent" effects. This was to be expected, as the effect of a polarizable continuum is due to simple electrostatics, in contrast to the ordering of various electromeric states, which is heavily dependent on electron correlation. Second, the primary effect of the polarizable continuum is to destabilize the iron(V)-oxo states with respect to the iron(IV)-oxo states. The effect is more pronounced for FeO(P)Cl and is essentially achieved already at the smaller value of the dielectric constant ($\varepsilon = 5.7$). Assuming that the "solvent" effect calculated at the DFT level is transferable to RASPT2 energetics, one would obtain the iron(IV)-oxo electromer as the ground state in FeO(P)Cl. The iron(V)-oxo electromer is predicted to be an excited state lying at only ∼4−6 kcal/mol above (depending on ε). In $FeO(P)^+$, the iron(V)-oxo electromer is still predicted to be the ground state, but the excited states of iron(IV)-oxo porphyrin radical character are expected at lower energies than *in vacuo*. In sum, the polarizable medium appears to be an important factor in determining the relative energetics of iron(IV)-oxo porphyrin radical and iron(V)-oxo electromers.

3.2. Cross-Checking the Methods for the Small Model. The studies on $FeO(P)^+$ and FeO(P)Cl have clearly demonstrated how much the calculated stabilities of various electromers are sensitive to the choice of methodology. Looking for further assessment of our computational methods, we focused on the small model, $FeO(L_2)^+$ ($L = \eta^2$-$N_2C_3H_5^-$). This model mimics the basic electronic features of the heme complexes but is, on the other hand, small enough to compare the results obtained from DFT and RASPT2 calculations with the CCSD(T) method. From an inspection of the various diagnostics of multireference effects in the coupled cluster wave function (see section 2 and the Supporting Information),[31,32,75,76] we conclude that the small model is still a well-behaving case for the CCSD(T) method. Therefore—as we have also taken care regarding the use of large enough basis sets—we believe that the CCSD(T) results given below may be considered reliable reference data.

Before discussing the stabilities of various electromeric states in the small model, let us first give an overview of the electronic states considered in the present study. The electronic situation of the small model is, obviously, slightly different from the heme complexes, because of the smaller size of the π system of L_2 as well as the lower symmetry. As for possible $(Fe^{IV}O)(L_2^{\bullet+})$ states, only those corresponding to the radical in the highest occupied b_2 π orbital of the ligand ($L_2^{\bullet+}b_2$) were calculated. Due to the lower (C_{2v}) symmetry, the Fe^VO doublet is no longer degenerate. Moreover, one of its components, $^2B_1$, strongly mixes with the $(Fe^{IV}O)(L_2^{\bullet+})$ doublet configuration of the same symmetry, thus producing a $^2B_1$ electronic state of mixed (Fe^V+Fe^{IV}) nature. In contrast, the other Fe^VO doublet state, $^2B_2$, remains predominantly iron(V)-oxo in character. The RASSCF calculations for the $^4Fe^V$ state (here, $^4A_2$) using the same active space as for the other electronic states were not successful due to unfavorable orbital rotations; for this reason, the result for this state will not be reported below (anyway, we believe that the results obtained for the other states already carry substantial information). In sum, the following electronic states have been studied for the small model:

$$(^3Fe^{IV}O)(^2L_2^{\bullet+}b_2) \rightarrow {}^4B_1$$

$$(^5Fe^{IV}O)(^2L_2^{\bullet+}b_2) \rightarrow {}^6B_2$$

$$(^3Fe^{IV}O)(^2L_2^{\bullet+}b_2) + (^2Fe^VO)(^1L_2) \rightarrow {}^2B_1$$

$$(^2Fe^VO)(^1L_2) \rightarrow {}^2B_2$$

Selected results obtained from the DFT, RASPT2, and CCSD(T) calculations are given in Table 5 (as for the heme complexes, all energies are given with respect to the triradicaloid state, $^4B_1$). The table includes two sets of RASPT2(23in22) results (the active space covering all π,π^* orbitals of L_2), obtained with two different basis sets: basis set II (i.e., the one used for the heme complexes in Tables 1 and 2) and the basis set Q/T (i.e., the one used in the CCSD(T) calculations). We note that both sets of RASPT2 energies agree very well. CCSD(T) relative energies are given for the Q/T basis as well as extrapolated to an infinite basis set on iron (∞/T). Also here, both sets of results are reasonably similar, suggesting that they are already converged with respect to the basis set.

Looking at Table 5, one should not forget that the bis(vinylogous amidine) ligand (L_2^{2-}) is obviously different from porphyrinate (P^{2-})—therefore, the stabilities of various electromeric states are also clearly different from those of the heme complexes. Nevertheless, the *trends* observed previously for the relative energies remain virtually the same. For instance, the nonhybrid functionals and RASPT2 predict the Fe^V ($^2B_2$) at much lower relative energy than the hybrid functionals. The same is also observed for the state of mixed Fe^V–Fe^{IV} character ($^2B_1$). The difference in the relative energies of ~10 kcal/mol between the B3LYP and BP86 is almost quantitatively comparable to that found previously for the heme models (cf. Tables 1 and 2). Moreover, the spin promotion energy ($^6B_2$–$^4B_1$) is much higher according to BP86 than according to B3LYP, B3LYP*, OLYP, and RASPT2. This is, again, in nearly quantitative agreement with the situation of the heme complexes. Thus, the overall similarity of the small model to the heme complexes justifies our choice of this system for testing various computational methodologies. It also suggests that the electronic structure issues discussed here and causing the discrepancies between different functionals are quite general features of high-valent iron-oxo complexes with π macrocycles. They are, apparently, not limited only to the special case of porphyrin.

Table 5. Relative Energies (kcal/mol) for the Low-Lying Electronic States of the Small Model, $FeO(L_2)^+$

						RASPT2[a]		CCSD(T)	
		B3LYP	B3LYP*	OLYP	BP86	II[b]	Q/T[b]	Q/T[b]	∞/T[b]
$(^3Fe^{IV})(^2L_2^{\bullet+})$	$^4B_1$	0.0	0.0	0.0	0.0	0.0	0.0	0.0	0.0
$(^5Fe^{IV})(^2L_2^{\bullet+})$	$^6B_2$	17.0	20.6	17.6	28.0	11.2	12.1	16.3	17.8
mixed[c]	$^2B_1$	1.5	−1.5	−8.6	−10.4	−12.2	−12.0	−8.9	−8.5
$(^2Fe^V)(^1L_2)$	$^2B_2$	8.8	5.6	−0.5	−2.7	−1.7	−2.1	−4.2	−3.7

[a] RAS(23in22) with RAS2(8+SO). [b] See the Supporting Information for a definition of the basis sets. [c] A mixture of doublet $(^3Fe^{IV})(^2L_2^{\bullet+})$ and $(^2Fe^V)(^1L_2)$ configurations.

When comparing the CCSD(T) and RASPT2 results, two observations may be made. First, RASPT2 most likely underestimates the spin promotion energy (overstabilizes the high-spin state) by some 4–6 kcal/mol, as was in fact expected (*vide supra*). This bias of RASPT2 in favor of the high-spin state is analogous to the one found previously in CASPT2 calculations of similar $d_{x^2-y^2} \rightarrow \sigma^*_{xy}$ spin-promotions in iron(II) complexes with N_4 and N_2O_2 ligands (e.g., heme, salen).[72−74] (N.B., also there, CCSD(T) calculations for small models were helpful to diagnose this effect.) For the present case, the spin promotion energy seems to be most correctly described by the B3LYP and OLYP functionals. The second important observation is that RASPT2 and CCSD(T) closely agree on the relative stability of the Fe^V and Fe^{IV} electromers. This is positive, providing extra credibility to this aspect of the RASPT2 energetics for the heme complexes. Thus, the CCSD(T) calculations for the small model indirectly support the previous conclusion about the low-lying iron(V)-oxo electromer in heme complexes.

3.3. Comparison with Experiment. As was already mentioned in the Introduction, the iron(IV)-oxo triradicaloid ground state is experimentally confirmed for enzymatic Cpd I species and their analogues, on the basis of a number of spectroscopic studies (UV/vis, NMR, EPR, resonance Raman, Mössbauer, X-ray absorption).[11−16,77−80] Recently, even the elusive Cpd I of cytochrome P450 has been isolated in high yield and characterized spectroscopically as an iron(IV)-oxo porphyrin radical species.[16] In view of the experimental consensus about the

iron(IV)-oxo porphyrin radical ground state for enzymatic Cpd I species and their synthetic analogues, the present prediction of low-lying iron(V)-oxo states from ab initio (RASPT2) calculations may be surprising and hard to believe. Even more, the calculations suggest an iron(V)-oxo ground state for both models, which seems to be contradicted by experimental results. However, when comparing the present calculations with experimental results, the following three factors should be taken into consideration.

First, even though the present RASPT2 calculations should be considered of high-quality—large basis sets and extensive active spaces were used, and the results obtained for the small model compare favorably to the CCSD(T) benchmark results—the calculated relative energies could still be in error by several kcal/mol. Uncertainties of such order may originate, for instance, from an unavoidable compromise between the size of the global active space and the size of the RAS2 subspace (for a discussion, see the Computational Details) as well as from the intrinsic approximations of RASPT2 theory. Because the various electromeric states are very close-lying, particularly for FeO(P)Cl, even a minor error in the calculated relative energies may easily change the character of the ground state to an iron(IV)-oxo porphyrin radical.

Second, the models studied here are clearly oversimplified and may not be directly comparable to experimentally investigated systems, the enzymes in particular. Moreover, the synthetic iron porphyrin complexes are based on porphyrin rings substituted at *meso* positions and some of them also at pyrrole β positions. The substituents, not included in the present models, may clearly affect the relative energy of iron(IV)-oxo porphyrin radicals and iron(V)-oxo states through their polar effect and/or by means of ruffling or saddling distortions of the porphyrin ring. The present choice of models was based on computational considerations, i.e., their high symmetry and relative simplicity, which are important factors in performing high-level ab initio calculations. This, in turn, is motivated by the main focus of the present study, which is benchmarking methods rather than making direct predictions about the situation in enzymes or for particular synthetic complexes.

Finally, the present calculations refer to isolated molecules *in vacuo*, while all known experiments probe the situation in solution or inside a protein pocket. On the basis of an implicit solvent model (COSMO), it was found here that the polarizable environment is an important factor favoring the iron(IV)-oxo porphyrin radical cation with respect to the iron(V)-oxo states. In fact, after considering the effect of a polar medium, the correct iron(IV)-oxo porphyrin radical ground state for FeO(P)Cl is recovered, in agreement with the experimental data for FeO(TMP)Cl (where TMP = tetramesitylporphyrin).[12,79,80] We further note that a qualitatively similar effect is known in P450 chemistry for iron species at one lower oxidation state (IV/III): the radical intermediate in the C−H hyrodoxylation mechanism has, *in vacuo*, a ground state with iron(IV) and a closed-shell porphyrin, $(P)Fe^{IV}(OH)/Alk^{\bullet}$ ($Alk^{\bullet}$ = alkyl radical). In contrast, the electromer with iron(III) and a porphyrin radical, $(P^{\bullet+})Fe^{III}(OH)/Alk^{\bullet}$, becomes most stable in a protein environment.[1]

Interestingly, the RASPT2 calculations for $FeO(P)^{+}$ point to an iron(V)-oxo ground state also in a polarizable medium. Even if, due to their limited precision (*vide supra*), these calculations may fail to predict the correct ground state of $FeO(P)^{+}$, theory seems to suggest that the "naked", five-coordinate cationic species, $FeO(P)^{+}$, has a stronger preference for the iron(V)-oxo state than the six-coordinated complex, FeO(P)Cl. In this regard, one may expect the actual coordination number of iron (five or six) to be an important experimental factor. Unfortunately, in many of the experimental studies dealing with complexes that are (formally) described as $FeO(TMP)^{+}$,[81−83] the actual ligation state of iron was not determined.[12] Since the chemical oxidants used to prepare the samples as well as the counterions from the iron(III) porphyrin substrates are potential axial ligands,[12] it is not clear whether the iron-oxo porphyrins probed in these experiments were isolated five-coordinate cations (thus comparable to the present five-coordinate model, $FeO(P)^{+}$) or six-coordinate complexes (thus more comparable to the present six-coordinate model, FeO(P)Cl). One should also notice that some five-coordinated iron-oxo porphyrin species were produced in gas-phase experiments, and their reactivity was characterized.[84,85] Although these species were tentatively assigned as iron(IV)-oxo porphyrin radical cations, their full spectroscopic characterization has not been performed, thus not permitting one to fully confirm this description.

The nature of the *ground state* has been quite firmly established for various Cpd I systems and their analogues. However, the character of the *low-lying excited states* and their potential role in multistate reactivity is less certain. The present theoretical study, likewise the previous one from the Jerusalem group,[24] clearly suggests that iron(IV)-oxo pentaradicaloid states and iron(V)-oxo states may be lying only a few kcal/mol above the triradicaloid ground state. Some recent experimental studies with the laser flash photolysis (LFP) technique[19] certainly go in this direction (note, however, a recent criticism of the LFP experiments for P450 and CPO enzymes[88−90]).

In particular, LFP experiments with metastable porphyrin-iron(IV) diperchlorates showed very reactive transients with oxo-transfer capabilities.[20,21] Although the full spectroscopic characterization (e.g., EPR, Mössbauer) of these short-living intermediates was not possible, they were tentatively identified as iron(V)-oxo porphyrin species, on the basis of their unique UV/vis spectrum and very high reactivity in oxo-transfer reactions.[21] Similar experimental data obtained from LFP experiments on iron corroles were also interpreted in terms of iron(V)-oxo corrole species.[91] Newcomb et al. further argue that the putative iron(V)-oxo electromer might be initially produced by heterolytic cleavage of the $FeO-ClO_3$ bond, with a kinetic barrier preventing it from immediate conversion (by internal electron transfer) to a more stable iron(IV)-oxo porphyrin radical species.[21,86] In this respect, they notice considerably high barriers for the analogous electronic isomerization of metastable $Fe^{IV}O(P)$ to more stable $Fe^{III}O(P^{\bullet+})$ species.[92]

According to the present theoretical study, the iron(V)-oxo electromer is a good candidate for the low-lying excited form of high valent iron-oxo porphyrins that might be observed in these experiments. The alternative candidate suggested by theory is a pentaradicaloid iron(IV)-oxo species. However, the UV/vis spectra of the short-living intermediates lack similarity to known spectra of porphyrin radical cations,[21] thus precluding this possibility and rather suggesting iron(V)-oxo character. The full interpretation of the LFP experiments[20,21,91] and determination of a possible role for the putative iron(V)-oxo species in catalysis would require more elaborate spectroscopic studies and further theoretical calculations. Clearly, even if an excited iron(V)-oxo electromer could be generated photochemically, this does not automatically mean that this species should also be involved in actual oxygenation pathways.[93] However, this intriguing proposition

should not be excluded solely on the basis of the very high energy found for the iron(V)-oxo species in previous B3LYP calculations.[2,23] The present study clearly indicates that this particular aspect of the energetics may not be well described by B3LYP and that the iron(V)-oxo states are expected at energies less than 10 kcal/mol above the ground state, even in a polar medium.

4. CONCLUSIONS

Two heme complexes with an iron-oxo group, $FeO(P)^+$ and FeO(P)Cl (P = porphin), were studied in this work, employing a number of DFT methods as well as second-order perturbation theory based on either Complete Active Space (CASPT2) and Restricted Active Space (RASPT2) wave functions. The aim was to provide an accurate description of the energetics of various electromeric states of the studied systems and to access the accuracy of the computational methods. Further calibration of the predicted energetics was carried out with respect to coupled cluster CCSD(T) calculations for the small model system, $FeO(L_2)^+$, containing two amidine ligands (η^2-$N_2C_3H_5^-$) instead of porphyrin.

The most important and intriguing suggestion from the present ab initio calculations undoubtedly concerns the presence of a low-lying iron(V)-oxo electromer. An iron(V)-oxo ground state is predicted by the present RASPT2 calculations for both heme models *in vacuo*. This is not consistent with the experimental observation of an iron(IV)-oxo porphyrin radical ground state in Cpd I species and their synthetic analogues.[11−15,77,78] However, it was found here that the presence of a polarizable medium (a solvent or protein environment) stabilizes the states with iron(IV)-oxo porphyrin radical character (by up to 8 kcal/mol) with respect to the iron(V)-oxo states. Upon considering this effect, the iron(IV)-oxo porphyrin radical electromer is predicted for FeO(P)Cl in agreement with experimental data of similar complexes,[12,79,80] but the iron(V)-oxo electromer is still low-lying and thermally accessible. A stronger preference for the iron(V)-oxo structure is predicted for the five-coordinate $FeO(P)^+$ cation without a *trans* axial ligand. A comparison between the RASPT2 and CCSD(T) results for the small model indicates that both methods provide a consistent picture of the relative energetics for iron(V)-oxo and iron(IV)-oxo electromers. Therefore, no large, systematic errors are to be expected in the RASPT2 energies for the heme complexes. However, uncertainties of several kcal/mol are very difficult to avoid in computational ab initio studies on such complicated systems. Even such small errors in the calculated energies may easily change the identity of the predicted ground state. A second important conclusion is that the high-spin (pentaradicaloid) form of the iron(IV)-oxo porphyrin radical electromer is also low-lying, most probably about 10 kcal/mol or less above the triradicaloid iron(IV)-oxo state. This conclusion is valid even though we believe (on the basis of the comparison with the coupled cluster calculations and on previous experience) that the CASPT2 and RASPT2 calculations may somewhat overestimate the stability of the high-spin state.

The role of the low-lying pentaradicaloid iron(IV)-oxo and the putative iron(V)-oxo electromer for mechanisms of catalytic reactions is currently under debate.[2,21,24,88,93] Computational studies have already shown that the pentaradicaloid states have a lower barrier for H-abstraction than the triradicaloids.[23,24,65] On the basis of experimental suggestions,[21] a similar enhanced reactivity was intuitively proposed for the excited iron(V)-oxo electromer, although such a proposal has so far not been definitely confirmed or rejected. The true role of the excited iron(V)-oxo electromers for catalytic properties of high-valent iron-oxo porphyrins and corroles remains to be addressed by further experimental and theoretical work. For further theoretical studies with DFT, it might be important to remember the dramatic difference between the hybrid and nonhybrid functionals in regard to (a) the spin promotion energy on the iron (i.e., difference in energy between tri- and pentaradicaloid iron(IV)-oxo states) and (b) the relative energy of the iron(V)-oxo vs iron(IV)-oxo porphyrin radical states. While comparison with ab initio calculations—in particular, with the CCSD(T) benchmark results for the small model—essentially confirms the high accuracy of hybrid functionals in predicting the spin promotion energy, these functionals seem to be much less accurate in describing the relative position of the iron(V)-oxo states. In fact, for the presently studied systems, it was quite difficult to find a single DFT method that describes both aspects of the energetics reasonably well (assuming, of course, that the present ab initio results are treated as a benchmark); among the functionals tested here, only OLYP points to relative energetics in accord with the ab initio picture.

We believe that the present study has also demonstrated some advantages of RASPT2 over standard CASPT2 calculations. The RASPT2 calculations performed in this study were based on a fairly large active space including not only all important orbitals on the FeO group but also a large number of porphyrin π orbitals and their correlating π^* orbitals. This is in contrast to the CASPT2 calculations where no more than just a few frontier orbitals of the porphyrin may be included in the active space (such like the Gouterman set of two π and two π^* orbitals). It turned out that the CASPT2 calculations cannot reliably reproduce (a) the splitting between a_{2u} and a_{1u} radicals on the porphyrin or (b) the magnetic coupling in the triradicaloid iron(IV)-oxo states. Both problems are readily solved in the present RASPT2 calculations with the larger active space. Furthermore, due to the better description of electron transfer from the iron to the porphyrin fragment, the relative energy of the iron(V)-oxo and iron(IV)-oxo ligand radical electromers is expected to be improved in the RASPT2 calculations. The RASPT2 method thus appears to be a promising tool for studying difficult cases with transition metals where very large active spaces may be unavoidable.

■ ASSOCIATED CONTENT

Supporting Information. Optimized Cartesian coordinates, additional DFT results, contour plots of the 29in28 active orbitals, more technical details and the test results obtained from CASSCF/CASPT2 and RASSCF/RASPT2 calculations. This material is available free of charge via the Internet at http://pubs.acs.org.

■ AUTHOR INFORMATION

Corresponding Author
*E-mail: mradon@chemia.uj.edu.pl.

■ ACKNOWLEDGMENT

This research project has been supported by grants from the Flemish Science Foundation (FWO), the Concerted Research Action of the Flemish Government (GOA), and the funds for

scientific research of the Ministry of Science and Higher Education of Poland (MNiSW; grant number N N204 333837). The computational grants from the Academic Computer Center in Kraków (CYFRONET) and in Gdańsk (CI TASK) are also acknowledged. Molecular graphics in Figure 2 were prepared with the XYZViewer program obtained from Sven de Marothy (Stockholm University).

REFERENCES

(1) Shaik, S.; Kumar, D.; de Visser, S. P.; Altun, A.; Thiel, W. *Chem. Rev.* **2005**, *105*, 2279–2328.
(2) Shaik, S.; Cohen, S.; Wang, Y.; Chen, H.; Kumar, D.; Thiel, W. *Chem. Rev.* **2010**, *110*, 949–1017.
(3) Pan, Z.; Zhang, R.; Newcomb, M. *J. Inorg. Biochem.* **2006**, *100*, 524–532.
(4) de Oliveira, F. T.; Chanda, A.; Banerjee, D.; Shan, X.; Mondal, S.; Lawrence Que, J.; Bominaa, E. L.; Münck, E.; Collins, T. J. *Science* **2007**, *315*, 835–838.
(5) Lee, S.; Han, J.; Kwak, H.; Lee, S.; Lee, E.; Kim, H.; Lee, J.; Bae, C.; Lee, S.; Kim, Y.; Kim, C. *Chem.—Eur. J.* **2007**, *13*, 9393–9398.
(6) Wasbotten, I.; Ghosh, A. *Inorg. Chem.* **2006**, *45*, 4910–4913.
(7) Dey, A.; Ghosh, A. *J. Am. Chem. Soc.* **2002**, *124*, 3206–3207.
(8) Ghosh, A. *J. Biol. Inorg. Chem.* **2006**, *11*, 712–724.
(9) It should be further noted that in the case of the P450 Cpd I, the ligand radical resides in a combination of a_{2u} with the σ orbital of sulphur from the axial cysteine. See, e.g., ref 1.
(10) Obviously, the term "porphyrin radical cation" and the notation "$P^{\bullet+}$" refer both to an open-shell porphyrin species with a charge of −1, as compared to a closed-shell porphyrin species with a charge of −2 (formally a porphyrinate anion). This notation is customary for high-valent metal-oxo species with noninnocent macrocyclic ligands—see for instance refs 2, 19−22, 24.
(11) Gold, A.; Weiss, R. *J. Porph. Phthal.* **2000**, *4*, 344–349.
(12) Weiss, R.; Bulach, V.; Gold, A.; Terner, J.; Trautwein, A. *J. Biol. Inorg. Chem.* **2001**, *6*, 831–845.
(13) Groves, J. T. *J. Inorg. Biochem.* **2006**, *100*, 434–447.
(14) Kim, S. H.; Perera, R.; Hager, L. P.; Dawson, J. H.; Hoffman, B. M. *J. Am. Chem. Soc.* **2006**, *128*, 5598–5599.
(15) Nam, W. *Acc. Chem. Res.* **2007**, *40*, 522–531.
(16) Rittle, J.; Green, M. T. *Science* **2010**, *330*, 933–937.
(17) Yamaguchi, K.; Watanabe, Y.; Morishima, I. *J. Chem. Soc., Chem. Commun.* **1992**, 1721–1723.
(18) Murakami, T.; Yamaguchi, K.; Watanabe, Y.; Morishima, I. *Bull. Chem. Soc. Jpn.* **1998**, *71*, 1343–1353.
(19) Zhang, R.; Newcomb, M. *Acc. Chem. Res.* **2008**, *41*, 468–477.
(20) Pan, Z.; Zhang, R.; Fung, L. W.-M.; Newcomb, M. *Inorg. Chem.* **2007**, *46*, 1517–1519.
(21) Pan, Z.; Wang, Q.; Sheng, X.; Horner, J. H.; Newcomb, M. *J. Am. Chem. Soc.* **2009**, *131*, 2621–2628.
(22) Ogliaro, F.; de Visser, S. P.; Groves, J. T.; Shaik, S. *Angew. Chem., Int. Ed.* **2001**, *40*, 2874–2878.
(23) Altun, A.; Shaik, S.; Thiel, W. *J. Am. Chem. Soc.* **2007**, *129*, 8978–8987.
(24) Chen, H.; Song, J.; Lai, W.; Wu, W.; Shaik, S. *J. Chem. Theory Comput.* **2010**, *6*, 940–953.
(25) Altun, A.; Kumar, D.; Neese, F.; Thiel, W. *J. Phys. Chem. A* **2008**, *112*, 12904–12910.
(26) Radoń, M.; Broclawik, E. *J. Chem. Theory Comput.* **2007**, *3*, 728–734.
(27) Schöneboom, J. C.; Neese, F.; Thiel, W. *J. Am. Chem. Soc.* **2005**, *127*, 5840–5853.
(28) Andersson, K.; Malmqvist, P.-Å.; Roos, B. O. *J. Chem. Phys.* **1991**, *96*, 1218–1226.
(29) Malmqvist, P.-Å.; Pierloot, K.; Shahi, A. R. M.; Cramer, C. J.; Gagliardi, L. *J. Chem. Phys.* **2008**, *128*, 204109.
(30) Pierloot, K.; Zhao, H.; Vancoillie, S. *Inorg. Chem.* **2010**, *49*, 10316–10329.
(31) Strickland, N.; Harvey, J. N. *J. Phys. Chem. B* **2007**, *111*, 841–852.
(32) Olah, J.; Harvey, J. *J. Phys. Chem. A* **2009**, *113*, 7338–7345.
(33) Ahlrichs, R.; Horn, H.; Schaefer, A.; Treutler, O.; Haeser, M.; Baer, M.; Boecker, S.; Deglmann, P.; Furche, F. *Turbomole v5.9*; Universitaet Karlsruhe; Karlsruhe, Germany.
(34) Frisch, M. J.; Trucks, G. W.; Schlegel, H. B.; Scuseria, G. E.; Robb, M. A.; Cheeseman, J. R.; Scalmani, G.; Barone, V.; Mennucci, B.; Petersson, G. A.; Nakatsuji, H.; Caricato, M.; Li, X.; Hratchian, H. P.; Izmaylov, A. F.; Bloino, J.; Zheng, G.; Sonnenberg, J. L.; Hada, M.; Ehara, M.; Toyota, K.; Fukuda, R.; Hasegawa, J.; Ishida, M.; Nakajima, T.; Honda, Y.; Kitao, O.; Nakai, H.; Vreven, T.; Montgomery, J. A., Jr.; Peralta, J. E.; Ogliaro, F.; Bearpark, M.; Heyd, J. J.; Brothers, E.; Kudin, K. N.; Staroverov, V. N.; Kobayashi, R.; Normand, J.; Raghavachari, K.; Rendell, A.; Burant, J. C.; Iyengar, S. S.; Tomasi, J.; Cossi, M.; Rega, N.; Millam, J. M.; Klene, M.; Knox, J. E.; Cross, J. B.; Bakken, V.; Adamo, C.; Jaramillo, J.; Gomperts, R.; Stratmann, R. E.; Yazyev, O.; Austin, A. J.; Cammi, R.; Pomelli, C.; Ochterski, J. W.; Martin, R. L.; Morokuma, K.; Zakrzewski, V. G.; Voth, G. A.; Salvador, P.; Dannenberg, J. J.; Dapprich, S.; Daniels, A. D.; Farkas, Ö.; Foresman, J. B.; Ortiz, J. V.; Cioslowski, J.; Fox, D. J. *Gaussian 09*, Revision A.1; Gaussian Inc.: Wallingford, CT, 2009.
(35) Weigend, F.; Ahlrichs, R. *Phys. Chem. Chem. Phys.* **2005**, *7*, 3297–3305.
(36) Becke, A. D. *J. Chem. Phys.* **1993**, *98*, 5648–5652.
(37) Perdew, J. P.; Ernzerhof, M.; Burke, K. *J. Chem. Phys.* **1996**, *105*, 9982–9985.
(38) Reiher, M.; Salomon, O.; Hess, B. A. *Theor. Chem. Acc.* **2001**, *107*, 48–55.
(39) Becke, A. D. *Phys. Rev. A* **1988**, *38*, 3098–3100.
(40) Perdew, J. P. *Phys. Rev. B* **1986**, *33*, 8822–8824.
(41) Perdew, J. P.; Burke, K.; Ernzerhof, M. *Phys. Rev. Lett.* **1996**, *77*, 3865–3868.
(42) Handy, N. C.; Cohen, A. *J. Mol. Phys.* **2001**, *99*, 403–412.
(43) Tawada, Y.; Tsuneda, T.; Yanagisawa, S.; Yanai, T.; Hirao, K. *J. Chem. Phys.* **2004**, *120*, 8425.
(44) Vydrov, O. A.; Scuseria, G. E. *J. Chem. Phys.* **2006**, *125*, 234109.
(45) Vydrov, O. A.; Heyd, J.; Krukau, A. V.; Scuseria, G. E. *J. Chem. Phys.* **2006**, *125*, 074106.
(46) Vydrov, O. A.; Scuseria, G. E.; Perdew, J. P. *J. Chem. Phys.* **2007**, *126*, 154109.
(47) Klamt, A. *J. Phys. Chem.* **1995**, *99*, 2224–2235.
(48) Cossi, M.; Rega, N.; Scalmani, G.; Barone, V. *J. Chem. Phys.* **2001**, *114*, 5691–5701.
(49) Karlström, G.; Lindh, R.; Malmqvist, P.-Å.; Roos, B.; Ryde, U.; Veryazov, V.; Widmark, P.-O.; Cossi, M.; Schimmelpfennig, B.; Neogrady, P.; Seijo, L. *Comput. Mater. Sci.* **2003**, *28*, 222−239; see: http://www.teokem.lu.se/molcas (accessed March 2011).
(50) Reiher, M.; Wolf, A. *J. Chem. Phys.* **2004**, *121*, 10945–10956.
(51) Ghigo, G.; Roos, B.; Malmqvist, P.-Å. *Chem. Phys. Lett.* **2004**, *396*, 142–149.
(52) Aquilante, F.; Malmqvist, P.-Å.; Pedersen, T. B.; Ghosh, A.; Roos, B. O. *J. Chem. Theory Comput.* **2008**, *4*, 694–702.
(53) Roos, B. O.; Lindh, R.; Malmqvist, P.-Å.; Veryazov, V.; Widmark, P.-O. *J. Phys. Chem. A* **2005**, *109*, 6575–6579.
(54) Pierloot, K.; Dumez, B.; Widmark, P.-O.; Roos., B. *Theor. Chim. Acta* **1995**, *90*, 87–114.
(55) Roos, B. O.; Andersson, K.; Fulscher, M.; Malmqvist, P.-Å.; Serrano-Andres, L.; Pierloot, K.; Merchan, M. Multiconfigurational perturbation theory: Applications in electronic spectroscopy. In *Advances in Chemical Physics: New Methods in Computational Quantum Mechanics*; Prigogine, I., Rice, S. A., Eds.; John Wiley & Sons: New York, 1996; Vol. 93.
(56) Pierloot, K. Nondynamic Correlation Effects in Transition Metal Coordination Compounds. In *Computational Organometallic Chemistry*; Cundari, T. R., Ed.; Marcel Dekker, Inc.: New York, 2001.
(57) Pierloot, K. *Mol. Phys.* **2003**, *101*, 2083–2094.
(58) Sauri, V.; Serrano-Andres, L.; Shahi, A. R. M.; Gagliardi, L.; Vancoillie, S.; Pierloot, K. *J. Chem. Theory Comput.* **2011**, *7*, 153–168.

(59) Werner, H.-J.; Knowles, P. J.; Manby, F. R.; Schütz, M.; Celani, P.; Knizia, G.; Korona, T.; Lindh, R.; Mitrushenkov, A.; Rauhut, G.; Adler, T. B.; Amos, R. D.; Bernhardsson, A.; Berning, A.; Cooper, D. L.; Deegan, M. J. O.; Dobbyn, A. J.; Eckert, F.; Goll, E.; Hampel, C.; Hesselmann, A.; Hetzer, G.; Hrenar, T.; Jansen, G.; Köppl, C.; Liu, Y.; Lloyd, A. W.; Mata, R. A.; May, A. J.; McNicholas, S. J.; Meyer, W.; Mura, M. E.; Nicklass, A.; Palmieri, P.; Püger, K.; Pitzer, R.; Reiher, M.; Shiozaki, T.; Stoll, H.; Stone, A. J.; Tarroni, R.; Thorsteinsson, T.; Wang, M.; Wolf, A. *MOLPRO*, version 2009. See http://www.molpro.net (accessed March 2011).

(60) de Jong, W. A.; Harrison, R. J.; Dixon, D. A. *J. Chem. Phys.* **2001**, *114*, 48–53.

(61) Dunning, T. H. *J. Chem. Phys.* **1989**, *90*, 1007–1023.

(62) Helgaker, T.; Klopper, W.; Koch, H.; Noga, J. *J. Chem. Phys.* **1997**, *106*, 9639–9646.

(63) Harvey, J. N.; Aschi, M. *Faraday Discuss.* **2003**, *124*, 129–143.

(64) Beran, G. J. O.; Gwaltneyb, S. R.; Head-Gordon, M. *Phys. Chem. Chem. Phys.* **2003**, *5*, 2488–2493.

(65) Chen, H.; Lai, W.; Shaik, S. *J. Phys. Chem. Lett.* **2010**, *1*, 1533–1540.

(66) Lee, T. J.; Taylor, P. R. *Int. J. Quantum Chem.* **1989**, *36*, 199–207.

(67) Janssen, C. L.; Nielsen, I. M. B. *Chem. Phys. Lett.* **1998**, *290*, 423–430.

(68) Ogliaro, F.; Cohen, S.; de Viser, S. P.; Shaik, S. *J. Am. Chem. Soc.* **2000**, *122*, 12892–12893.

(69) Harvey, J. N. *Annu. Rep. Prog. Chem., Sect. C: Phys. Chem.* **2006**, *102*, 203–226.

(70) Pierloot, K.; Vancoillie, S. *J. Chem. Phys.* **2006**, *125*, 124303.

(71) Pierloot, K.; Vancoillie, S. *J. Chem. Phys.* **2008**, *128*, 034104.

(72) Kepenekian, M.; Robert, V.; Le Guennic, B. *J. Chem. Phys.* **2009**, *131*, 114702.

(73) Radoń, M.; Broclawik, E.; Pierloot, K. *J. Phys. Chem. B* **2010**, *114*, 1518–1528.

(74) Vancoillie, S.; Zhao, H.; Radoń, M.; Pierloot, K. *J. Chem. Theory Comput.* **2010**, *6*, 576–582.

(75) Neogrády, P.; Medveď, M.; Černušák, I.; Urban, M. *Mol. Phys.* **2002**, *100*, 541–560.

(76) Karton, A.; Rabinovich, E.; Martin, J. M. L.; Ruscic, B. *J. Chem. Phys.* **2006**, *125*, 144108.

(77) Groves, J. T.; Haushalter, R. C.; Nakamura, M.; Nemo, T. E.; Evans, B. J. *J. Am. Chem. Soc.* **1981**, *103*, 2884–2886.

(78) Hosten, C. M.; Sullivan, A. M.; Palaniappan, V.; Fitzgerald, M. M.; Terner, J. *J. Biol. Chem.* **1994**, *269*, 13966–13978.

(79) Gross, Z.; Nimri, S. *J. Am. Chem. Soc.* **1995**, *117*, 8021–8022.

(80) Wolter, T.; Meyer-Klaucke, W.; Müther, M.; Mandon, D.; Winkler, H.; Trautwein, A. X.; Weiss, R. *J. Inorg. Biochem.* **2000**, *78*, 117–122.

(81) Mandon, D.; Weiss, R.; Jayaraj, K.; Gold, A.; Bill, E.; Trautwein, A. X. *Inorg. Chem.* **1992**, *31*, 4404–4409.

(82) Müuther, M.; Bill, E.; Trautwein, A. X.; Mandon, D.; Weiss, R.; Gold, A.; Jayaraj, K.; Austin, R. N. *Hyperfine Interact.* **1994**, *91*, 803–808.

(83) Jones, R.; Jayaraj, K.; Gold, A.; Kirk, M. L. *Inorg. Chem.* **1998**, *37*, 2842–2843.

(84) Crestoni, M. E.; Fornarini, S. *Inorg. Chem.* **2007**, *46*, 9018–9020.

(85) Chiavarino, B.; Cipollini, R.; Crestoni, M.; Fornarini, S. *J. Am. Chem. Soc.* **2008**, *130*, 3208–3217.

(86) Sheng, X.; Horner, J. H.; Newcomb, M. *J. Am. Chem. Soc.* **2008**, *130*, 13310–13320.

(87) Wang, Q.; Sheng, X.; Horner, J. H.; Newcomb, M. *J. Am. Chem. Soc.* **2009**, *131*, 10629–10636.

(88) Rittle, J.; Younker, J. M.; Green, M. T. *Inorg. Chem.* **2010**, *49*, 3610–3617.

(89) Yuan, X.; Sheng, X.; Horner, J. H.; Bennett, B.; Fung, L. W.-M.; Newcomb, M. *J. Inorg. Biochem.* **2010**, *104*, 1156–1163.

(90) It must be noted here that the LFP experiments for cytochrome P450 and CPO enzyme (refs 86, 87) have been recently criticized (refs 88, 89) as not generating Cpd I despite the initial claims of the authors. In these studies, an enzyme was treated first with peroxynitrite to generate Cpd II, and subsequent photooxidation was (incorrectly) expected to yield Cpd I. However, in this study, we mostly refer to other LFP experiments to which the recent criticism does not seem to apply—namely, the study described in refs 20 and 21. This study was carried out not for an enzyme but for a small biomimetic complex, and it employed a different oxidant agent, namely, iron(III) perchlorate. Moreover, the intermediate species was not a Cpd II analogoue but an iron(IV) porphyrin diperchlorate, whose subsequent LFP gave a short-living transient that was tentatively assigned as iron(V)-oxo porphyrin perchlorate (cf. refs 20, 21). We believe that the criticism of some LFP experiments expressed by Green et al. (ref 88) remains specific to those experiments with enzymes, while LFP in general remains a well-estabilished technique for generating high-valent metal-oxo complexes and for studying their reactivity (cf. ref 19).

(91) Harischandra, D.; Zhang, R.; Newcomb, M. *J. Am. Chem. Soc.* **2005**, *127*, 13776–13777.

(92) Pan, Z.; Harischandra, D. N.; Newcomb, M. *J. Inorg. Biochem.* **2009**, *103*, 174–181.

(93) de Montellano, P. R. O. *Chem. Rev.* **2010**, *110*, 932–948.